ASME Journal of Tribology
Online journal at:
https://asmedigitalcollection.asme.org/tribology

Optimization and Dynamic Modeling of Friction Losses in Reciprocating Diesel Engines With Emphasis on Rod-Crank Geometry and Ring–Cylinder Contact

Luca Piancastelli
Department of Industrial Engineering (DIN),
University of Bologna—Alma Mater Studiorum,
Bologna 40136, Italy
e-mail: luca.piancastelli@unibo.it

Irene Giusti[1]
Department of Industrial Engineering (DIN),
University of Bologna—Alma Mater Studiorum,
Bologna 40136, Italy
e-mail: irene.giusti4@unibo.it

Marella De Santis
Department of Industrial Engineering (DIN),
University of Bologna—Alma Mater Studiorum,
Bologna 40136, Italy
e-mail: marella.desantis2@unibo.it

This technical report presents a physics-based model to quantify frictional power losses in a reciprocating diesel engine, focusing on the effects of the connecting-rod-to-crank-radius ratio (L/r) and piston-ring contact area. Simulations were performed for three L/r ratios (2.43, 3.2, and 3.59) and three ring configurations: a single 1.25 mm ring; two rings of 1.25 mm and 1.5 mm; and three rings of 1.25 mm, 1.5 mm, and 1.5 mm. Results indicate that frictional power increases with contact area, from 102 W (single ring, $L/r = 3.59$) to 326 W (three rings, $L/r = 2.43$). Shorter rods amplify lateral forces and friction, whereas longer rods reduce losses with diminishing returns. Normalization against the baseline two-ring case (187 W) highlights these trends. The model identifies an optimal configuration at a moderate L/r ratio with two rings of balanced thickness, minimizing energy loss while maintaining ring durability and sealing performance. [DOI: 10.1115/1.4071486]

Keywords: piston ring wear, rod-to-crank ratio, internal combustion engine, tribological modeling, contact pressure, wear-rate analysis, contact area

1 Introduction

Frictional losses in reciprocating internal combustion engines account for a significant portion of total mechanical losses, influencing fuel efficiency, emissions, and component longevity. In diesel engines, the piston–cylinder assembly represents a primary source of tribological interaction: piston rings maintain sealing and load support but also generate additional frictional work. Accurate quantification of these losses is important for guiding design decisions, including geometry selection, material choice, and surface treatment [1,2].

Previous studies have investigated piston-ring friction using experimental measurements and analytical models. Empirical correlations typically relate frictional torque to ring tension, surface roughness, lubrication regime, and sliding speed, while mechanistic models consider hydrodynamic film formation and asperity contact [3–5]. However, many existing approaches simplify the piston–ring interface by considering only a single ring or neglect the influence of connecting-rod geometry on piston kinematics.

The connecting-rod-to-crank-radius ratio (L/r) directly affects piston motion, altering the magnitude and timing of lateral forces on the ring package. Shorter rods increase side loads and can lead to uneven lubrication, whereas longer rods reduce lateral forces but may introduce constraints related to engine packaging and mass [6]. Similarly, the number and thickness of piston rings determine the total contact area, influencing hydrodynamic pressure distribution, asperity contact, and overall friction. While additional rings improve sealing and reduce blow-by, they also increase frictional drag.

This technical report develops a physics-based model to investigate how L/r and piston-ring contact area affect frictional power losses. The study considers multiple connecting-rod ratios and ring configurations across a full engine cycle. The objectives are to (i) quantify variations in instantaneous and integrated frictional power, (ii) identify trends relative to a baseline two-ring configuration, (iii) assess tradeoffs between friction reduction and practical design constraints, and (iv) provide guidelines for selecting connecting-rod lengths and ring geometries in diesel engine design.

2 Materials and Methods

This section presents the engine configuration, piston ring materials, surface treatments, friction modeling, and numerical procedure adopted in this work. All parameters and methods are selected to support the analysis of frictional losses as a function of piston-ring contact area and connecting-rod-to-crank-radius ratio (L/r).

2.1 Engine Geometry and Operating Conditions. The engine analyzed in this study is a common rail diesel engine with a stroke of 90.4 mm. Key geometric and operating parameters, including contact pressure, sliding velocity, lubricant viscosity, surface roughness, oil film thickness, lubrication parameter, and friction coefficient, are reported in Table 1. The cylinder bore diameter is denoted as D, the connecting-rod length as L, and the crank radius as r. The engine is equipped with one to three piston rings depending on the configuration considered, and the engine speed selected for the analysis is 3800 rpm.

The ratio of connecting-rod length to crank radius, L/r, is varied to study its influence on piston kinematics and frictional losses. Two limiting values, 2.43 and 3.59, are considered together with an intermediate configuration corresponding to the original engine design, $L/r = 3.2$. These values correspond to the extreme cases observed in high-performance engines, such as Formula 1 and World Superbike units [7–9].

[1]Corresponding author.

Contributed by Tribology Division of ASME for publication in the JOURNAL OF TRIBOLOGY. Manuscript received January 22, 2026; final manuscript received March 19, 2026; published online April 10, 2026. Assoc. Editor: Robert L. Jackson.

Table 1 Representative friction parameters in reciprocating engines

Parameter	Symbol	Typical range
Contact pressure	p	1–5 MPa
Sliding velocity	v	1–25 m/s
Lubricant viscosity	η	0.002–0.01 Pa·s
RMS roughness	σ	0.2–0.6 μm
Oil film thickness	$h_{\min}$	0.3–1.5 μm
Lubrication parameter	Λ	0.5–4.0
Friction coefficient	μ	0.001–0.15

The maximum piston velocity as a function of crank angle θ is determined from the kinematic relationship of the crank-slider mechanism

$$v_{\text{pist}}(\theta) = \omega r\left(\sin\theta + \frac{\sin 2\theta}{2n}\right) \tag{1}$$

where $\omega = 2\pi\text{rpm}/60$ represents the angular velocity of the crankshaft, and $n = L/r$ is the rod-to-crank ratio.

2.2 Piston Ring Materials and Surface Treatments. Piston rings are designed to provide sufficient elasticity, corrosion resistance, and wear resistance under severe engine operating conditions. The most commonly used materials are gray cast iron, in lamellar or nodular form and either annealed or non-annealed [10,11], and steel, typically martensitic chrome steel or spring steel that has undergone nitriding to improve surface hardness and durability.

To further enhance tribological performance, piston ring surfaces are often treated or coated. Thermal-spray molybdenum and galvanic chromium coatings improve wear resistance and emergency running behavior [12,13]. Advanced composite coatings, including chrome-ceramic and diamond-coated layers, embed hard particles in a metallic matrix to achieve ultra-low friction and long-lasting durability. Physical vapor deposition coatings, such as CrN, are commonly applied to compression and oil control rings, providing high surface hardness and smoothness to reduce friction over the ring lifetime.

Additional surface treatments, including phosphating and copper plating, are employed primarily to improve corrosion resistance. Phosphate coatings produce a matte black, rust-resistant surface, while copper plating protects against burn marks during running-in without affecting the functional performance of the ring [14].

2.3 Friction Force Modeling. The friction force between piston rings and cylinder liner is expressed as

$$F_f = \mu A_c p \tag{2}$$

where p is the local contact pressure, A_c the effective contact area, and μ the coefficient of friction. The coefficient of friction depends on the lubrication regime, surface roughness, lubricant viscosity, and temperature.

2.3.1 Lubrication Regimes. Three lubrication regimes are considered: boundary, mixed, and hydrodynamic [15], characterized by the dimensionless parameter Λ

$$\Lambda = \frac{h_{\min}}{\sigma}, \quad \sigma = \sqrt{\sigma_1^2 + \sigma_2^2} \tag{3}$$

Classification of regimes:

- $\Lambda < 1$: boundary
- $1 \le \Lambda < 3$: mixed
- $\Lambda \ge 3$: hydrodynamic

Typical friction parameters for reciprocating engines are given in Table 1, and lubrication regimes during operation are summarized in Table 2.

2.3.2 Hydrodynamic Friction

$$\mu = \frac{C\eta v}{pR} \tag{4}$$

where η is the lubricant viscosity, v is the sliding velocity, p is the contact pressure, R is the effective radius of curvature, and C is an empirical temperature-dependent coefficient

$$C(T) = C_0 + \beta(T - T_0) \tag{5}$$

where C_0 is the coefficient at the reference temperature T_0, β is the temperature sensitivity coefficient, and T is the lubricant temperature.

2.3.3 Mixed and Boundary Friction. In mixed lubrication

$$\mu = \mu_0\left(\frac{\eta v_p}{p_c h}\right)^n \tag{6}$$

where μ_0 is a reference friction coefficient, v_p is the piston sliding velocity, p_c is the contact pressure, h is the lubricant film thickness, and n is an empirical exponent.

In boundary lubrication

$$\mu = \mu_s + K p_c \tag{7}$$

where μ_s is the boundary friction coefficient and K is a proportionality constant relating friction to contact pressure.

2.4 Numerical Procedure for Friction Work. The indicated pressure–volume (PV) diagram of the commercial common rail diesel engine considered in this study is shown in Fig. 1. The instantaneous gas pressures extracted from this cycle are used as input for evaluating the piston lateral forces and the resulting frictional interaction between the piston ring pack and the cylinder liner throughout the engine cycle.

The instantaneous friction work per crank angle increment is

$$dW_i = F_{f,i} \cdot s_i \tag{8}$$

The total work per engine cycle is obtained by summing all increments

Table 2 Comparison of lubrication regimes in piston ring–cylinder liner contact

Parameter	Boundary	Mixed	Hydrodynamic
Oil film thickness h	<0.1 μm	0.1–2 μm	> 2 μm
Contact type	Asperity contact	Partial film	Full film
Load support	Solid contact	Solid + fluid	Fluid only
Friction mechanism	Adhesion, plowing	Mixed	Viscous shear
Typical friction coefficient μ	0.1–0.2	0.01–0.08	0.002–0.01
Heat generation	High	Moderate	Low
Wear-rate	High	Medium	Low

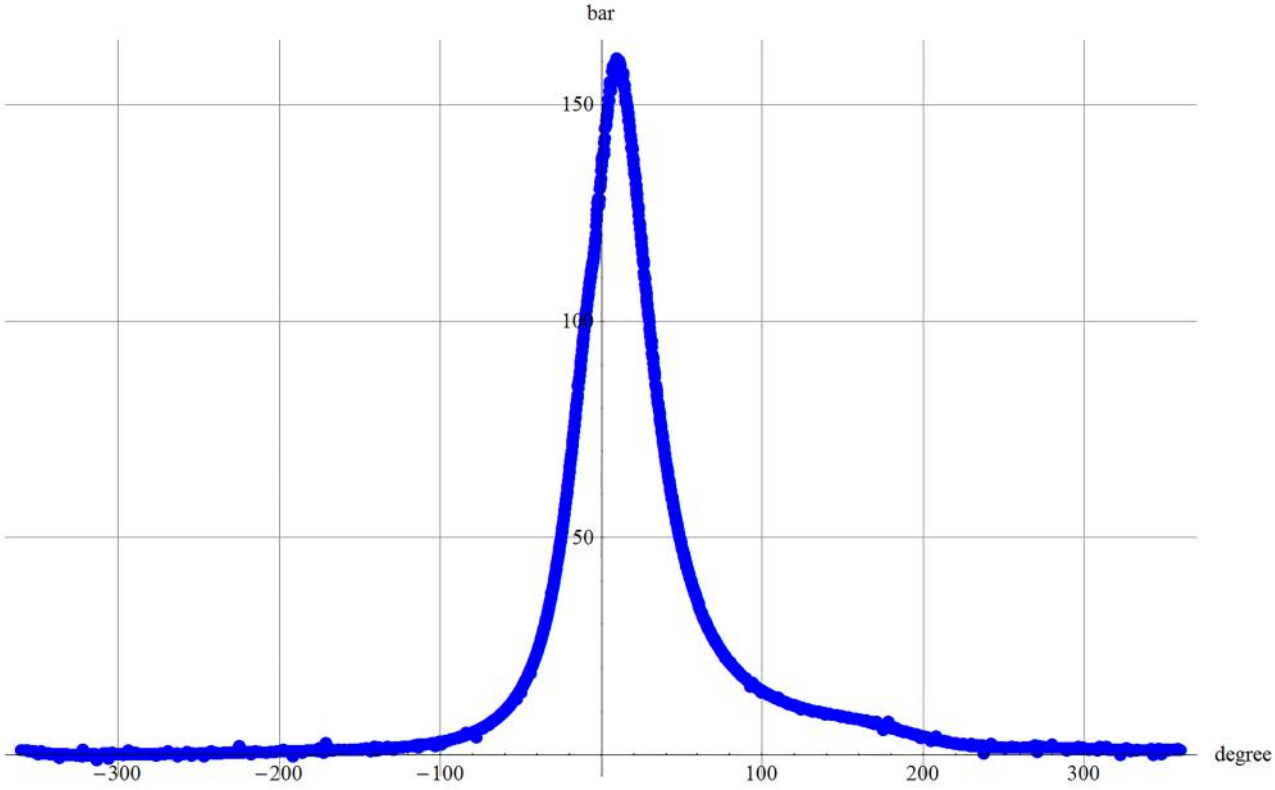

Fig. 1 Pressure–volume diagram of the commercial common rail diesel engine used as input for the friction analysis

$$W_f = \sum_{i=1}^{N} dW_i \tag{9}$$

where s_i is the piston displacement increment at crank angle α_i, and $N \approx 7200$ steps ($\Delta\alpha = 0.1$ deg) over a full crank revolution.

2.5 Piston Ring Contact Area and Configuration. The effective contact area between the piston ring pack and the cylinder liner depends on the number of rings and their axial widths. For n rings with widths w_i, the total contact area is computed as

$$A_{\text{contact}} = \sum_{i=1}^{n} w_i \cdot D \tag{10}$$

Equation (10) represents the nominal geometric contact area between the piston rings and the cylinder liner. In practice, the real-microscopic contact area is smaller than the nominal one because contact occurs at discrete asperities on the interacting surfaces. The real area of contact therefore depends on surface roughness characteristics such as asperity radius, root-mean-square (RMS) roughness, and asperity density. In the present model, the nominal contact area is adopted as an effective macroscopic parameter to describe the ring–liner interface. The influence of surface roughness and asperity-scale interactions is implicitly accounted for through the empirical friction correlations used in the hydrodynamic, mixed, and boundary lubrication regimes described in the previous section.

Table 3 Power dissipated (W) as a function of number of segments and connecting-rod ratio

	Conrod length/Crank radius		
# Segments	2.43	3.2 (Original)	3.59
1	149	104	102
2	280	187	185
3	326	286	284

The current engine configuration employs two rings ($w_1 = 1.25$ mm, $w_2 = 1.5$ mm). In order to evaluate the influence of ring pack design on frictional losses, alternative configurations with one, two, and three rings are also considered.

The analyzed piston ring configurations are defined as follows:

(1) Single-ring configuration ($w_1 = 1.25$ mm);
(2) Two-ring configuration corresponding to the original engine design ($w_1 = 1.25$ mm, $w_2 = 1.5$ mm);
(3) Three-ring configuration ($w_1 = 1.25$ mm, $w_2 = 1.5$ mm, $w_3 = 1.5$ mm).

In addition, three values of the connecting-rod-to-crank-radius ratio are analyzed ($L/r = 2.43$, 3.2, and 3.59). All combinations of piston ring configurations and L/r ratios are evaluated in the numerical simulations, and the resulting frictional power dissipation is presented and discussed in Sec. 3.

3 Results and Discussion

3.1 Reference Engine Cycle. The indicated PV diagram of the commercial common rail diesel engine considered in this study is shown in Fig. 1. This cycle was used as the reference for computing piston lateral forces and the corresponding frictional work at the piston–ring cylinder interface. The instantaneous gas pressures extracted from this PV diagram provide the input for evaluating the variation of contact pressures along the stroke and the resulting frictional losses.

3.2 Effect of Connecting-Rod Length on Friction. The influence of the connecting-rod-to-crank-radius ratio (L/r) on frictional power losses is summarized in Tables 3 and 4. The results

Table 4 Normalized power dissipated (%) relative to original configuration with two segments (187 W = 100%)

	Conrod length/Crank radius		
# Segments	2.43	3.2 (Original)	3.59
1	79.7	55.6	54.5
2	149.7	100.0	98.9
3	174.3	152.9	151.9

demonstrate that shorter rods ($L/r = 2.43$) generate higher lateral forces, resulting in increased frictional losses compared to the original engine configuration ($L/r = 3.2$) and the long-rod configuration ($L/r = 3.59$). This trend is consistent across all tested piston ring configurations.

Increasing L/r reduces the deviation from harmonic piston motion and lowers peak piston velocity, which in turn diminishes side forces and friction. However, the marginal benefit of increasing L/r beyond the original design is limited, as the reduction in friction is small relative to the additional constraints on engine size, weight, and packaging.

3.3 Influence of Piston Ring Contact Area. The number and axial width of piston rings strongly affect the total contact area and the resulting frictional losses at the piston–cylinder interface. The piston ring configurations analyzed in this study are defined in Sec. 2.5, where the contact area formulation and the considered ring pack geometries are described.

As shown in Table 3, frictional power dissipation increases substantially with the number of rings. For instance, at the original L/r ratio of 3.2, the dissipated power increases from 104 W for a single-ring configuration to 187 W for two rings and 286 W for three rings.

The normalized values reported in Table 4 further highlight the relative increase in friction associated with the larger contact area produced by additional rings.

These results emphasize the classical tradeoff between sealing performance and frictional losses. Increasing the number of rings improves blow-by control and mechanical robustness, but it also increases the frictional drag at the ring–liner interface. Conversely, reducing the ring count lowers friction but may compromise durability and sealing effectiveness.

3.4 Combined Effect of L/r and Ring Configuration. The combined analysis of connecting-rod length (L/r) and piston-ring contact area, as reported in Tables 3 and 4, shows that the highest frictional losses occur when a short rod ($L/r = 2.43$) is paired with three rings, reaching 326 W. This result reflects the synergistic effect of increased lateral forces and a larger contact area. In contrast, long rods ($L/r = 3.59$) with a two-ring configuration achieve frictional power nearly identical to the original engine configuration (185 W versus 187 W) while simultaneously reducing side loads and potential wear. Configurations with a single ring consistently yield the lowest frictional losses; however, they may not meet durability and blow-by requirements.

These results confirm the expected tradeoff in design: achieving optimal friction reduction requires a careful balance between the connecting-rod-to-crank-radius ratio and the number and thickness of piston rings.

3.5 Discussion. The results demonstrate that piston friction depends not only on ring material or lubrication but also significantly on engine geometry and ring pack design. Adjusting the connecting-rod-to-crank-radius ratio (L/r) or modifying the number of piston rings can reduce friction; however, practical constraints such as engine size, weight, sealing requirements, and wear considerations limit the extent of these optimizations.

This study also emphasizes the value of a physics-based, cycle-resolved model. By using the real-engine PV diagram (Fig. 1) as input, transient effects in piston motion and friction are captured, particularly near top dead center and bottom dead center, where velocity gradients and lubrication regimes change rapidly.

The findings indicate that a configuration with two rings combined with an intermediate L/r ratio, corresponding to the original engine design, provides a reasonable compromise between minimizing friction and maintaining durability. Increasing L/r beyond conventional limits offers only marginal friction reduction, while employing more than two rings significantly increases friction with minor improvements in wear or sealing. These insights can be directly applied to the design and optimization of ring pack geometry and connecting-rod length to achieve the best tradeoff between mechanical efficiency and operational reliability.

4 Conclusions

The study demonstrates that the tribological performance of a reciprocating diesel engine is strongly influenced by both the connecting-rod length and the piston ring configuration. The mathematical model, based on the indicated pressure cycle (Fig. 1), captures the effects of L/r and piston-ring contact area on instantaneous and integrated frictional power losses.

The results show that increasing the number of piston rings significantly raises frictional losses due to the larger contact area. While additional rings can improve sealing and wear performance, the incremental benefit diminishes beyond two rings, whereas frictional losses continue to increase. Similarly, short connecting rods (low L/r) generate higher lateral forces, increasing friction, whereas longer rods reduce these side loads. However, the reduction in friction becomes marginal for very high L/r ratios, and further increases are constrained by engine packaging, mass, and cost considerations.

Configurations with a single ring yield the lowest frictional losses but may compromise sealing and durability, whereas configurations with three rings produce substantially higher friction due to the increased contact area. Consequently, a moderate L/r combined with a two-ring configuration provides a reasonable compromise between frictional efficiency and component durability.

Overall, these findings provide practical guidance for engine designers in selecting connecting-rod length and piston ring configuration to optimize tribological performance and overall mechanical efficiency.

Conflict of Interest

There are no conflicts of interest.

Data Availability Statement

No data, models, or code were generated or used for this article.

Nomenclature

h = oil film thickness (m)
n = rod-to-crank ratio, L/r
p = local contact pressure (Pa)
v = sliding velocity (m/s)
C = empirical constant for hydrodynamic friction
D = cylinder bore diameter (m)
K = empirical constant for boundary friction
L = connecting-rod length (m)
R = effective radius of curvature of the piston–ring interface (m)
T = temperature (K)
h_{min} = minimum oil film thickness (m)

p_c = characteristic contact pressure for mixed/boundary lubrication (Pa)
s_i = piston displacement increment at crank angle α_i (m)
v_{pist} = instantaneous piston velocity (m/s)
$v_{\max}$ = maximum piston velocity (m/s)
w_i = axial width of piston ring i (m)
A_c = effective piston ring contact area (m^2)
F_f = friction force (N)
W_f = total friction work per engine cycle (J)
dW_i = incremental friction work at step i (J)

Greek Symbols

α = crank angle (deg)
η = lubricant dynamic viscosity (Pa·s)
Λ = lubrication parameter, film thickness-to-roughness ratio
μ = coefficient of friction
μ_0 = reference friction coefficient in the mixed regime
μ_s = friction coefficient in the boundary regime
σ = combined RMS surface roughness of contacting surfaces (m)
σ_1, σ_2 = RMS roughness of ring and cylinder surfaces (m)
ω = crankshaft angular velocity (rad/s)

References

[1] Holmberg, J., Ronkainen, H., Laukkanen, A., and Wallin, K., 2007, "Friction and Wear of Coated Surfaces: Scales, Modelling and Simulation of Tribomechanisms," Surf. Coat. Technol., **202**(4–7), pp. 1034–1049.
[2] Blau, P. J., 2009, *Friction Science and Technology: From Concepts to Applications*, 2nd ed., CRC Press, Boca Raton, FL.
[3] Dowson, D., 1998, *History of Tribology*, 2nd ed., Wiley, Chichester, UK.
[4] Wakuri, Y., Hamatake, T., Soejima, M., et al., 1992, "Piston ring friction in internal combustion engines," Tribol. Int., **25**(5), pp. 299–308.
[5] Falco, S., Bianchi, A., and Rossi, L., "Experimental Investigation of Piston Ring Friction." Technical Report 2015-01-0387, SAE Technical Paper, 2015.
[6] Heywood, J. B., 2018, *Internal Combustion Engine Fundamentals*, 2nd ed., McGraw-Hill, New York.
[7] Jia, D., Liu, Y., Lei, J., Deng, X., Deng, W., and Ji, H., 2025, "Design and Kinematic Characterization of Connecting Rod Set for Variable Compression Ratio Engines," Energies, **18**(5), p. 1276.
[8] Khudhair, M. R., Kamil, F., Kadhom, M. A., and Gburi, F. H., 2024, "Optimum Design of Connecting Rod – A Review," J. Mech. Des. Vib., **11**(1), pp. 1–9.
[9] Boretti, A. A., and Cantore, G., 2000, "Similarity Rules and Parametric Design of Race Engines," SAE International, **109**, pp. 775–787.
[10] Demarchi, V., and Vatavuk, J., "Nitrided Gray Cast Iron Piston Rings," Technical Report 942393, SAE Technical Paper, 1994.
[11] Sokolov, O. D., Mannapova, O. V., Kostrzhytskyi, A. I., and Olik, A. P., 2006, "Enhancement of Corrosion Resistance of Gray Cast Iron by Ion Nitriding," Mater. Sci., **42**(6), pp. 849–852.
[12] Araujo, J. A., and Marques, G. A., 2010, "Engineered PVD CRN Coatings for Piston Ring Application," Proceedings of 53rd Society of Vacuum Coaters Technical Conference, Orlando, FL, Apr. 17–22, pp. 307–312.
[13] Rozario, A., Baumann, C., and Shah, R., 2019, "The Influence of a Piston Ring Coating on Wear and Friction During Linear Oscillation," Lubricants, **7**(1), p. 8.
[14] Hutchinson, J., 1983, "Hydrodynamic Lubrication of Piston Ring Packs," ASME J. Lubr. Tech., **105**(1), pp. 14–20.
[15] Stephan, S., Schmitt, S., Hasse, H., and Urbassek, H. M., 2023, "Molecular Dynamics Simulation of the Stribeck Curve: Boundary Lubrication, Mixed Lubrication, and Hydrodynamic Lubrication on the Atomistic Level," Friction, **11**(12), pp. 2342–2366.